

Impact of the environment on a hygrometry sensor response

Marianne SAGNARD*, Thierry LAROCHE†, Jean-Michel FRIEDT* and Sylvain BALLANDRAS†

* Femto-ST, Time and frequency department

15B av. des Montboucons 25000 BESANCON

Email: marianne.sagnard@frecnsys.fr, jmfriedt@femto-st.fr

†Frec'n'sys

18 rue Alain Savary 25000 BESANCON

Email: thierry.laroche@frecnsys.fr, sylvain.ballandras@frecnsys.fr

Abstract—The measure of hygrometry is a current approach for soil monitoring in geophysical applications. In that case, *in-situ* subsurface earth moisture control is tackled with the design of wireless and free from battery sensors interrogated from the surface. Since the most significant impact of humidity on ground physical properties is on the relative permittivity ε_r , the measurement is based on the capacitive pulling of an acoustic resonator. The connection of a variable capacitance in parallel with an antenna feeding the resonator with incoming power induces losses and hence, range losses through capacitive short circuit under strong moisture contents.

Consequently, an alternative solution is considered. It consists in the design of a coupled resonator in which antenna and sensor (capacitive load) are electrically separated and linked by the acoustic field confined in the cavity between the electrodes forming the two ports. When probed by a Ground Penetrating RADAR, the echo delay, or in the case of a resonator, the frequency difference between the two modes is expected to depend on the humidity level.

Thus, this study is dedicated to the understanding of the impact of humidity on the different elements of sensor. This work also designs a surface acoustic wave resonator to convey the signal. In such a way, this work exhibits that under ideal load the set-up above mentioned indeed allows the measure of ε_r due to capacitive pulling, leading to a wired hygrometer. Then, the possibility to carry out wireless sensing using an antenna both as an antenna and as a sensitive area is explained.

I. INTRODUCTION

Passive sensors interrogated through a wireless link from the surface are ideally suited for subsurface physical and chemical sensing. Indeed, the lack of local energy source is consistent with the inaccessibility of the sensor once installed for any maintenance or battery replacement purpose. Acoustic transducers based on elastic waves guided in solids, used as intrinsic sensors, take advantage of the dependence of the parametric sensitivity on their physical characteristics (particularly the phase velocity) to environmental changes. More specifically, Surface Acoustic Wave (SAW) sensors based on this feature have been developed for temperature and stress remote sensing [1]. Such an approach however restricts the measured quantities to those impacting the acoustic wave characteristics, preventing the measurement of other specific properties. For example, to estimate the *in-situ* soil humidity, hygrometry sensors have to be developed. These zones are hard to access so wireless and remotely controlled sensors are preferably

selected with respect to the classical time-domain reflectometry measurement (TDR) requiring an operator and the insertion of a probe in soil. Moreover, the SAW sensor can't be immersed in wet places. Consequently, innovative measurement means, such as the modification of electric boundary conditions using resistive or capacitive loads, must be elaborated.

Thus, a complementary approach consists in the use of an acoustic transducer as a radiofrequency transponder whose first port is connected to an antenna for wireless communication, and whose second port is connected to a load designed to change the basic operation mode of the device (for instance, mode coupling in longitudinally coupled resonator filter - LCRF) so that the returned signal conveys the load sensor environmental condition [2], [3]. If both of them are buried with the acoustic transducer, varying soil moisture will then affect both antenna and load impedance. Therefore, the arising question is how to separate both contributions and to prevent the symmetrical design of the transponder from being similarly affected on both ports by permittivity ε_r changes.

In addition, the use of an only coupled mode resonator allows a differential measurement while avoiding the use of several single port resonators that can couple one another and age in a different way along time, leading to the degradation of the sensor response.

In that purpose, this work focuses on the analysis of the response variations of a sensor composed of an antenna, a SAW LCRF and a sensitive zone, under the fluctuation of soil hygrometry as was experimentally addressed in [4]. In this way, a SAW device is designed and electrical equivalent circuits are used to represent the sensitive area and the antenna. The first step of this paper is to explain how antenna and sensing load parameters evolve under a change of ε_r . Indeed, the variation of soil humidity induces a fluctuation of ε_r . Consequently, the capacitive load used in the considered sensor changes too. Moreover, as mentioned above, antenna is also impacted by the soil moisture.

The first part of this paper then is dedicated to the study of the sensor component parameter variations with ε_r . Then, resonant frequency variations under the modification of electrical conditions (due to the presence of antenna and/or sensitive zone) is pointed out and discussed. Finally, the application presented in this work could be developed according to the sensitivity to the environment obtained on a specific SAW

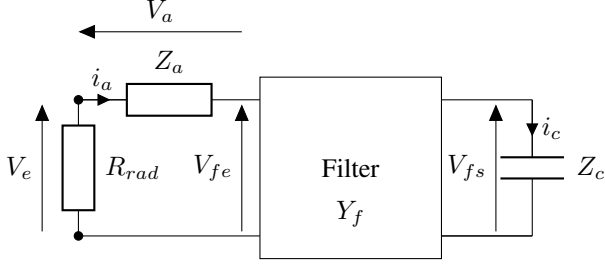


Figure 1. Illustration of an hygrometry sensor. It is composed of an antenna (Z_a and R_{rad}), of a SAW LCRF (Filter, Y_f) and of a capacitance (load, C_l). The output voltage V_e is measured at the terminals of R_{rad} .

design on Lithium Niobate.

II. OPERATING OF A HYGROMETRY SENSOR

This section explains the working principle of hygrometers based on surface acoustic waves. The sensor is at first sketched then its frequency response defined.

A. Basic diagram of the hygrometry sensor

Hygrometers that take advantage of guided waves in solids are composed of three parts:

- 1) A sensitive zone that measures the variation of soil humidity ;
- 2) A SAW filter, that conveys the signal ;
- 3) An antenna to communicate with an interrogator.

The sensitive zone is connected to the SAW device whose admittance is Y_f . The change in soil humidity affects the behavior of the sensor while the SAW transponder relays the signal to the antenna. The drawing of the system is represented figure 1.

The sensitive zone is, in first approach, assumed to be a pure capacitance C_l of impedance Z_c (also called "load" in this paper). However, it would be easy to consider an RLC circuit instead of a unique capacitance to take into account the inductive behavior of the component and also losses due to the wire bonding. The antenna is modeled by a impedance Z_a and a radiative resistance R_{rad} connected in series with the SAW filter. On figure 1, V_e (resp. V_a) is the voltage at the terminals of the radiative resistance (resp. antenna impedance) ; V_{fe} (resp. V_{fs}) is the input (resp. output) voltage of the filter. i_a and i_c are the currents that cross Z_a and the load C_l .

B. Frequency response of the sensor

Three cases are studied to understand the behavior of the sensor and to point out the contribution of each part of the device:

- 1) the system composed of the filter and of the capacitance. There is no antenna in this model (fig. 2(a));
- 2) the antenna and the filter are considered (fig. 2(b));
- 3) the behavior of the whole structure (antenna, filter and load) is investigated (fig. 1).

Each above mentioned items can be described by an equivalent electrical matrix which are described in the next sections. These matrices are cascaded to obtain the performance of the sensor [5].

1) *Filter and capacitance (fig. 2(a))*: The purpose is to find the link between V_{fe} and i_a taking into account Z_c and the components of $[Y_f]$.

The equations establishing the behavior of this first sub-system are :

$$\begin{cases} \begin{pmatrix} i_a \\ -i_c \end{pmatrix} = [Y_f] \begin{pmatrix} V_{fe} \\ V_{fs} \end{pmatrix} = \begin{bmatrix} Y_{f11} & Y_{f12} \\ Y_{f21} & Y_{f22} \end{bmatrix} \begin{pmatrix} V_{fe} \\ V_{fs} \end{pmatrix} \\ V_{fs} = Z_c i_c \end{cases} \quad (1)$$

From (1) and (2), i_a can be written as follow :

$$i_a = (Y_{f11} - Z_c \frac{Y_{f12}Y_{f21}}{1 + Z_c Y_{f22}}) V_{fe} \quad (3)$$

The term in brackets in (3) is the admittance at the input of the system.

2) *Antenna and filter (fig. 2(a))*: In the same way that in the previous paragraph, the behavior of the filter loaded by its antenna is determined. The system behaves following these equations:

$$\begin{cases} V_{fe} = V_e - V_a \\ V_a = i_a Z_a \\ i_a = Y_{f11} V_{fe} + Y_{f12} V_{fs} \\ i_s = -i_c = Y_{f21} V_{fe} + Y_{f22} V_{fs} \end{cases} \quad (4)$$

The injection of expressions of (4) and (5) in (6) leads to:

$$i_a = \frac{Y_{f11}}{1 + Z_a Y_{f11}} V_e + \frac{Y_{f12}}{1 + Z_a Y_{f11}} V_{fs} \quad (8)$$

Then, the previous equation is implemented in (7) :

$$i_s = \frac{Y_{f21}}{1 + Y_{f11} Z_a} V_e + (Y_{f22} - \frac{Y_{f12} Y_{f21} Z_a}{1 + Z_a Y_{f11}}) V_{fs} \quad (9)$$

The admittance matrix of the antenna-filter ensemble consequently reads:

$$[Y_{AF}] = \begin{bmatrix} \frac{Y_{f11}}{1 + Z_a Y_{f11}} & \frac{Y_{f12}}{1 + Z_a Y_{f11}} \\ \frac{Y_{f21}}{1 + Y_{f11} Z_a} & (Y_{f22} - \frac{Y_{f12} Y_{f21} Z_a}{1 + Z_a Y_{f11}}) \end{bmatrix} \quad (10)$$

3) *Whole system (antenna, filter and capacitance, fig. 1)*: If the previous results are gathered, the admittance at the input of the whole system is obtained:

$$i_a = (Y_{AF11} - Z_c \frac{Y_{AF12} Y_{AF21}}{1 + Z_c Y_{AF22}}) V_e \quad (11)$$

where Y_{AFij} (subscripts i and $j \in \llbracket 0, 1 \rrbracket$) are the components of the admittance tensor Y_{AF} .

This admittance (in brackets) is the figure of merit of the system. From this quantity, we are able to know the behavior of the device and to draw, if needed, the S_{11} parameter (which is the effective value an electronic system will read).

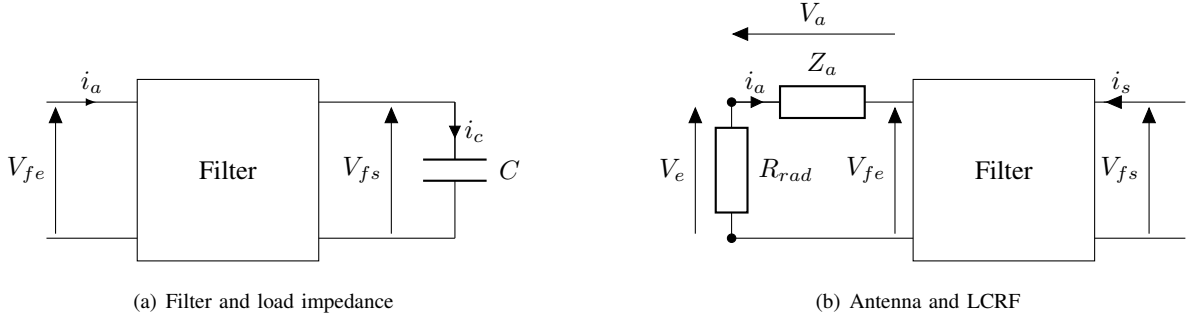


Figure 2. Diagram of the elements of the considered hygrometry sensor

The behavior of a passive and remotely controlled sensor based on the use of a unique SAW resonator is now defined considering (11). Consequently, the next section concentrates on the impact of soil humidity on both sensitive zone (which must be emphasized) and antenna (which should not have any influence on the device frequency response).

III. VARIATION OF THE ELECTRICAL PARAMETERS OF THE LOAD AND OF THE ANTENNA WHEN SOIL HUMIDITY CHANGES

As mentioned in Introduction, antenna and load are both submitted to the variation of humidity when dived in the ground. This section details their parameter dependence on soil hygrometry, and *de facto* the evolution of (11). Indeed, it is essential to understand how each part of the device reacts independently to allow for distinguishing the contribution of each element in the sensor response.

Moreover, soil humidity can be characterized through the relative permittivity ε_r . Actually, in air $\varepsilon_r = 1$ whereas it varies from 3 to 30 when the ground passes from dry to wet [6]. The following paragraph is devoted to the establishment of the link between ε_r and the elements of the antenna and the load.

A. Variation of the capacitance under hygrometry variations

The load C_l (of impedance $Z_c = \frac{1}{jC_l\omega}$, ω the angular frequency) is related to ε_r through the following equation:

$$C_l = \varepsilon_0 \varepsilon_r \times \left(\frac{A}{d} \right)_l \quad (12)$$

where $\varepsilon_0 = 8.854187 \times 10^{-12} \text{ F/m}$ is the vacuum permittivity and $(A/d)_l$ the ratio area of the capacitor on width of the dielectric between the armatures. In the previous equation, C_l only depends on ε_r ; $(A/d)_l$ is fixed as a virtual geometric parameter and calculated below.

In dry earth, $\varepsilon_r = 3$ and C_l is arbitrarily dimensioned to be equal to 4 pF (this could be dealt in depth in further investigations). As a consequence, $(A/d)_l$ is deduced as follows:

$$\left(\frac{A}{d} \right)_l = \frac{C_l}{\varepsilon_0 \varepsilon_r} = \frac{4 \times 10^{-12}}{8.854187 \times 10^{-12} \times 3} = 0.15059 \text{ m} \quad (13)$$

From (12) and (13), it is easy to determine that the capacitance is in the range [4pF ; 40pF] when buried in the ground.

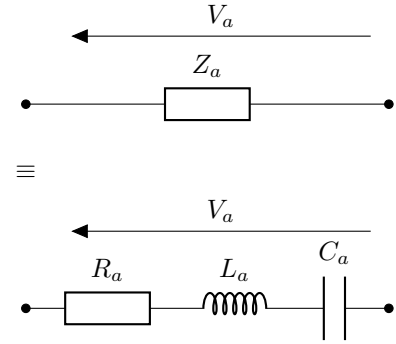


Figure 3. Equivalent circuit of the antenna without the radiative part

B. Antenna model and its variations versus soil humidity

A dipole antenna whose frequency resonance is 434 MHz (to interrogate in the industrial, scientific and medical ISM band) is used in this application. It is dimensioned to be a half wavelength antenna so the length of its wires is $l_w = 17.5 \text{ cm}$. Its quality factor Q is assumed to be around 10 and its radiative resistance is equal to $\simeq 73.5 \Omega$ [7].

This kind of antenna can be modeled by an RLC circuit connected in series with the SAW filter (figure 3). As a consequence, Z_a reads:

$$Z_a = R_a + j \left(L_a \omega - \frac{1}{C_a \omega} \right) \quad (14)$$

where R_a represents the losses due to the Joule effect, L_a is the inductance due to the wires of the antenna and C_a its capacitance. The pulsation ω is equal to $2\pi f$ with f the current frequency. R_a and L_a are intrinsic parameters of the antenna.

Let us note that the geometric parameter $(A/d)_a$ is, like in the previous section, a fixed parameter. At first, R_a , L_a and $(A/d)_a$ are defined by studying the antenna in air. Then, the dependence of C_a (so, Z_a) on ε_r is examined.

1) *Antenna inductance L_a* : L_a directly stems from the geometry of the antenna :

$$L_a = \mu_0 \times 2l_w = 0.43 \mu \text{H} \quad (15)$$

with $\mu_0 = 4\pi \cdot 10^{-7} \text{ H/m}$ the permeability of the vacuum.

2) *Loss resistance R_a* : R_a is the resistance due to Joule effect in the wires of the antenna. Considering its material (Copper) and its dimensions, R_a is found equal to:

$$R_a = \frac{\rho \times 2l_w}{S} = 7.5m\Omega \quad (16)$$

assuming that $\rho = 1.7 \times 10^{-8} \Omega.m^{-1}$ the resistivity of Copper and S the section of the wire whose diameter is 1mm. It should be noticed that the skin effect could have been taken into account to adopt the point of view of antenna specialists. However, considering the resistance of a wire has got no impact on the conclusion of this work and makes easier the understanding of this paragraph.

3) *Antenna capacitance C_a* : The first step of the paragraph is to defined the virtual geometric constant $(A/d)_a$ of the antenna capacitance. For that, the value of the antenna capacitance is at first defined in the air: $C_{a/air}$. Then, the relations governing the behavior of *RLC* circuit are used to calculate $(A/d)_a$. Finally, the evolution of C_a versus ε_r is established.

In series RLC circuits, inductance and capacitance are derived from the resonance frequency f_r . Indeed, the magnitude of the impedance Z_a is minimum at f_r . Therefore:

$$L_a C_a \times (2\pi f_r)^2 = 1 \quad (17)$$

In air, the capacitance of the antenna $C_{a/air}$ is consequently equal to:

$$C_{a/air} = \frac{1}{L_a \times (2\pi f_r)^2} = 0.30576pF \quad (18)$$

From (12) and (18) :

$$\left(\frac{A}{d}\right)_a = \frac{C_{a/air}}{\varepsilon_0 \varepsilon_r} = 0.034533m \quad (19)$$

Finally, the evolution of C_a versus ε_r is the following :

$$C_a = \left(\frac{A}{d}\right)_a \varepsilon_0 \varepsilon_r = 0.034533\varepsilon_0 \varepsilon_r \quad (20)$$

4) *Antenna response versus ε_r* : All the antenna parameters are now known. Consequently, its frequency response can be plotted. Figure 4 points out the frequency shift of the antenna admittance Y_a when ε_r increases. Note that in this paragraph the behavior of the whole antenna (R_{rad} in series with Z_a) is examined. The dipole antenna used in this work is a half wavelength antenna, so its radiation resistance is equal to 73.5Ω [7]. The antenna resonance falls from 434 MHz to 79 MHz when the permittivity varies from 1 (air) to 30 (humid ground). As a consequence, the sensor will not operate above the antenna resonance but on its side. This could be an advantage to restrain the influence of the antenna on the system.

IV. DESIGN OF THE FILTER

The choice to design a SAW LCRF (cf. fig 5) for this application was made to be close to the conditions described in reference [3]. Moreover, the coupling between the two modes is mandatory for the filter to act as a transponder and to

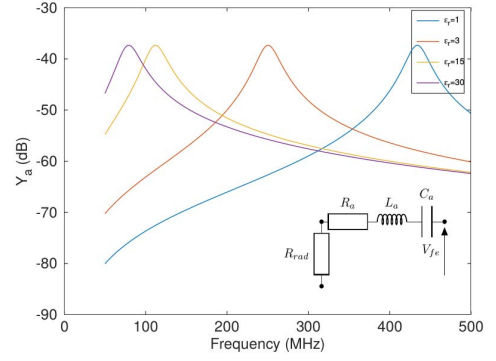


Figure 4. Evolution of the frequency response of the antenna when ground hygrometry varies

TABLE I. SUMMARY OF THE DIMENSIONS OF THE SAW LCRF

	number of strips	p (μm)	a/p
Mirrors	480	4.42	0.5
Transducers	60	4.40	0.4
Coupler	100	4.42	0.5

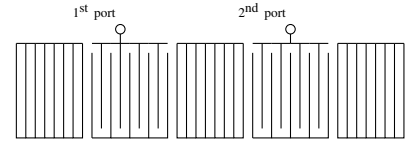


Figure 5. Diagram of a LCRF

transmit energy (so, information) from one port to another (i.e. from the load to the antenna).

Because of internal requirements, the device is made on (YXl)/128° Lithium Niobate cut. A 350 nm thick Aluminum layer is deposited at the surface of the substrate to form the electrodes. The dimensions of this component are summarized in table I. The frequency response of the device can consequently be analyzed. s_{11} parameter and y_{11} admittance are then plotted on figure 6. They give several information. Firstly, the two modes are located at 433.546 MHz and at 434.188 MHz. Moreover, despite the high coupling factor of the Lithium Niobate and thanks to a source removal, a low coupling factor (resp. 0.08% and 0.171%) is achieved with spectral purity. Finally, the second resonance is perfectly adapted to 50Ω : the considered frequency corresponds to a real mode and the minimum of s_{11} is located at the resonance (for another configuration, this particular point could correspond to another impedance) whereas the first mode is lightly shifted from this working point.

In brief, the SAW transponder is now designed to operate in the considered ISM band.

V. EVOLUTION OF THE FREQUENCY RESPONSE OF THE DEVICE VS SOIL HYGROMETRY

The behavior of each part of the system has just been studied. We now focus on the behavior of the antenna and/or the load connected to the filter.

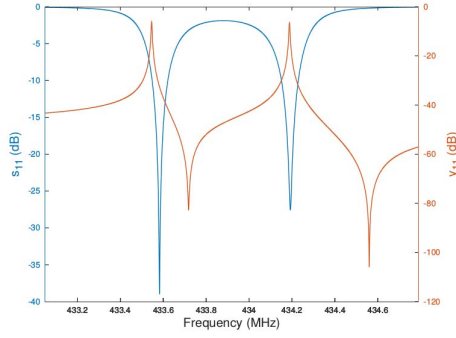


Figure 6. Frequency response of the SAW filter without the antenna or the capacitance. Its admittance Y_{11} and its parameter S_{11} are represented

A. Capacitance and filter for wired sensing

At first, the case of figure 2(a) is examined. Knowing that the permittivity of the ground varies from 3 to 30, the response of the filter connected to the sensitive zone under this fluctuation is clarified. The results are reported on figure 7. The first observation that can be done is the decrease of the frequency resonances when C_l increases. Namely, the wetter the soil, the lower the frequency resonances. In fact, the first mode varies from 433.607 MHz to 433.555 MHz corresponding to a frequency shift of 52 kHz. As for the second mode, its resonance frequency experiences a 76 kHz shift (from 434.275 to 434.199 MHz). Moreover, figure 8 displays the evolution of each resonance frequency versus ϵ_r . Each mode has got its own behavior, so differential measurements can be done. This is also put forward on figure 9 that plots the frequency difference between the two modes (frequencies f_1 and f_2): when ϵ_r increases, the quantity $\Delta f = f_2 - f_1$ (in kHz) evolves according to:

$$\Delta f = 668.13 + 98.25 \times \left(\frac{1}{\epsilon_r} - \frac{1}{3}\right) + 60.372 \times \left(\frac{1}{\epsilon_r} - \frac{1}{3}\right)^2 \quad (21)$$

Consequently, the *filter capacitance* system can already be used as a wired hygrometer.

Two remarks can be added:

- the results are consistent with the results of publication [3] ;
- it seems that the larger the mode coupling, the larger the frequency shift.

This paragraph confirmed that the evolution of soil humidity can be monitored using the system of figure 2(a). The next step is to focus on the influence of the hygrometry on the filter response when it is connected to the antenna. By this way, the design of a wireless hygrometer is getting closer.

B. Antenna and filter system behavior

We proceed using the same methodology than in the previous section to determine the behavior of the *antenna-filter* system when $\epsilon_r \in [3; 30]$. The response of this structure is plotted on figure 10. The antiresonance seems to appear before the resonance, which is not possible if the different elements are correctly connected to each other (absence of short-circuit).

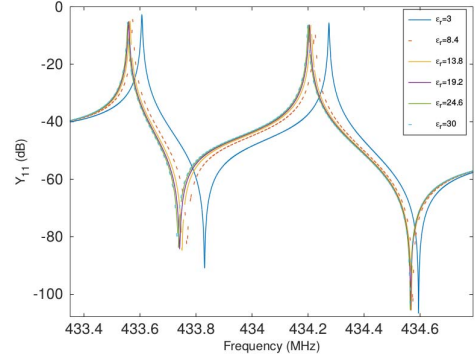


Figure 7. Evolution of the frequency response of the system represented fig. 2(a) when ϵ_r varies from 3 to 30

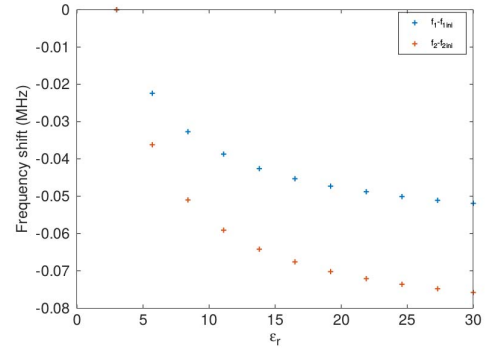


Figure 8. Evolution of the two resonance frequencies when the humidity of the soil varies. The second frequency (higher frequency) decreases faster than the first one (lower frequency)

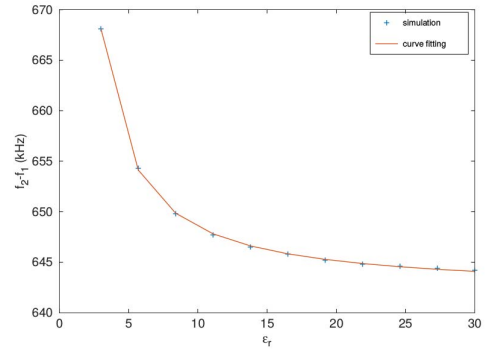


Figure 9. Evolution of the frequency difference $f_2 - f_1$ in the ground

Hence, the studied frequency range is widened and the evolution of ϵ_r is restricted from 1 to 1.20. Actually, the lowering of the range of ϵ_r allows for the understanding of the behavior of the *antenna-filter* system along relative permittivity. Figure 11 displays a sizable decrease of the resonance frequencies. The frequency shift is high enough to make the first mode out of the mirror Bragg band, which leads to a loss of the first mode signature and to the location of the second mode just after the first antiresonance. No influence is seen on the antiresonances. At last, the resonances vary so much that we are no more able to determine the value of ϵ_r by monitoring the resonances, before even the flooding of the sensor into the ground.

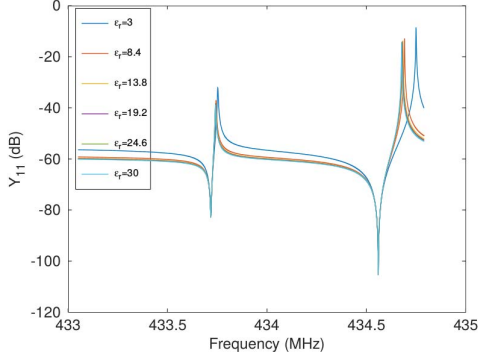


Figure 10. Evolution of the frequency response of the system represented fig. 2(b) when ϵ_r varies from 3 to 30

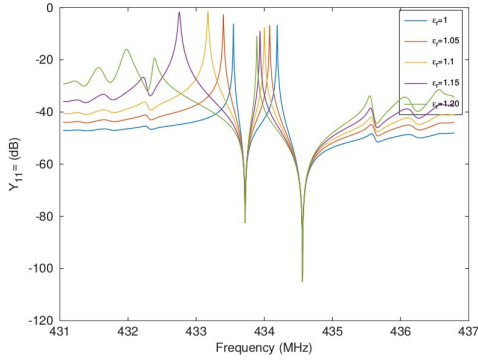


Figure 11. Evolution of the frequency response of the system represented fig. 2(b) when ϵ_r varies from 1 to 1.20

However, in this narrow permittivity range, the different behaviors of the two modes versus ϵ_r are clearly visible: figure 11 shows a larger impact of ϵ_r on the first mode than on the second one. Next part is consequently dedicated to the exploiting of this particularity.

C. Antenna and filter as a wireless hygrometry sensor

The previous paragraphs pointed out the impact of humidity (through ϵ_r) on the response of the filter loaded by an antenna. Particularly, ϵ_r influences the value of the capacitance of the dipole antenna (see section II-B2). C_a modifications involve the shifting of the two resonances of the LCRF connected to the antenna with a larger impact on the first one than on the second mode (see section V-B).

Figure 12 shows the variation of both modes when $\epsilon_r \in [1, 1.20]$: the first frequency resonance decreases of more than 1 MHz in this range whereas the second one is reduced of about only 200 kHz. Then, figure 13 makes visible the increase of the frequency difference $\Delta f = f_2 - f_1$ when relative permittivity increases too. This quantity can be estimated as follow:

$$\Delta f(\text{MHz}) = 0.64677 - 0.75019(\epsilon_r - 1) + 23.6655(\epsilon_r - 1)^2 + 29.91453(\epsilon_r - 1)^3 \quad (22)$$

As a consequence, the possibility to conduct a differential measurement has been brought to light. Namely, the antenna

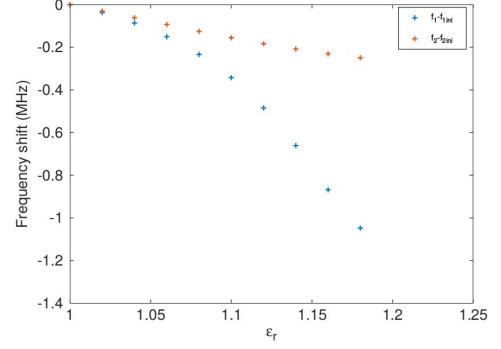


Figure 12. Evolution of the frequency shifts of the filter loaded by its antenna when relative permittivity varies from 1 to 1.20

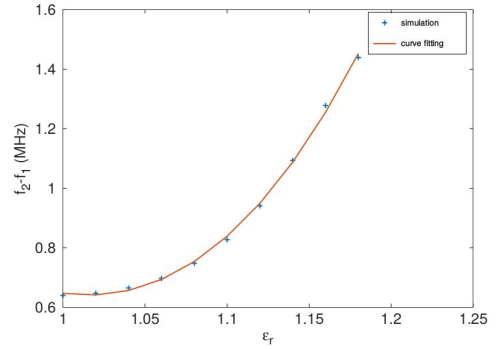


Figure 13. Evolution of the frequency difference $f_2 - f_1$ when relative permittivity varies from 1 to 1.20

forms both the interrogation part (emission and reception of the signal) and the sensitive area of the hygrometer.

VI. CONCLUSION

In order to develop a ground hygrometry sensor, the impact of humidity on the different elements of the system is studied. The sensor is in first instance composed of three parts :

- a sensitive zone to measure the variation of soil hygrometry ;
- a filter acting as a transponder ;
- an antenna.


This paper shows that the sensitive zone, modeled for now by a pure capacitance, varies from 4 to 40 pF linearly with ϵ_r (so, with the hygrometry). In further works, the load capacitance will be replaced by an impedance composed of fixed resistive and inductive parts that are distinctive features of the component, and of a capacitance whose value depends on earth hygrometry. As for the antenna, the large impact of ground ϵ_r on its frequency response is pointed out. Indeed, the dipole antenna, which can be modeled by an RLC circuit sees its frequency resonance collapse of 355 MHz with the increase of humidity. A SAW filter (LCRF type) is also designed on Lithium Niobate to work in the ISM band centered on 434 MHz.

Then, the effective impact of the humidity on the response of the *filter load* system is demonstrated: the variation of

several dozen of kHz on each mode is sufficient enough to calibrate the sensor and to measure the ground humidity. Actually, a wired hygrometer has been modeled. Regarding the influence of the antenna on the sensor, its huge sensitivity on environmental parameters is pointed out to the extent that a slight variation of ε_r make the signal out of the frequency range of interest. As a consequence, the study of this system is done for a variation of the permittivity comprised between 1 and 1.20 instead of from 3 to 30. This last point reveals that the two modes are impacted by the variation of antenna parameters (particularly, its capacitance due to ε_r changes) and that they behave differently. The shift of the frequency difference can be estimated with a third degree interpolation function. Consequently, a measure of relative permittivity can be carry out using the antenna, both to convey the signal and to be the sensor itself. By this way, a wireless hygrometry measurement can be conducted.

In future works, the SAW filter presented in this work will be manufactured to carry out calculation/test correlations and if needed, to adjust the model and to refine the design. The modification of the design of the SAW component is also considered to lower the impact of ε_r on the sensor response and consequently, to be able to measure soil humidity with the device presented in this article.

ACKNOWLEDGMENT

 We are grateful to the DGA and to the ANRT for their financial backings.

REFERENCES

- [1] A. Kawalec and M. Pasternak. A New High-Frequency Surface Acoustic Wave Sensor for Humidity Measurement. *IEEE Transactions on Instrumentation and Measurement*, 57(9):2019–2023, Sept 2008.
- [2] L. Reindl, C. C. W. Ruppel, A. Kirmayr, N. Stockhausen, M. A. Hilhorst, and J. Balendonck. Radio-requestable passive SAW water-content sensor. *IEEE Transactions on Microwave Theory and Techniques*, 49(4):803–808, Apr 2001.
- [3] T. Laroche, G. Martin, W. Daniau, S. Ballandras, J. M. Friedt, and J. F. Leguen. A coupled-mode filter structure for wireless transceiver-sensors using reactive loads. In *2012 IEEE International Frequency Control Symposium Proceedings*, pages 1–6, May 2012.
- [4] J. M. Friedt. Passive cooperative targets for subsurface physical and chemical measurements. In *2016 16th International Conference on Ground Penetrating Radar (GPR)*, pages 1–6, June 2016.
- [5] T. Laroche, J. Garcia, E. Courjon, S. Ballandras, and W. Daniau. A comprehensive model of the electrical response of SAW devices submitted to thermal perturbation. In *2014 European Frequency and Time Forum (EFTF)*, pages 71–74, June 2014.
- [6] R.A van Overmeeren, S.V Sariowan, and J.C Gehrels. Ground penetrating radar for determining volumetric soil water content; results of comparative measurements at two test sites. *Journal of Hydrology*, 197(1–4):316–338, 1997.
- [7] Constantine A. Balanis. *Antenna Theory: Analysis and Design*. John Wiley & Sons, February 2016.